

Burr Distribution Describes Ultrasound Speckle Statistics of Soft Biological Tissues

Sedigheh S. Poul

Department of Mechanical Engineering,
University of Rochester,
Rochester, New York, United States
poul@rochester.edu
(ORCID: 0000-0002-9582-3004)

Stefanie J. Hollenbach

Department of Obstetrics and Gynecology,
University of Rochester Medical Center,
Rochester, New York, United States
stefanie_hollenbach@urmc.rochester.edu
(ORCID: 0000-0001-9135-5090)

Kevin J. Parker

Department of Electrical and Computer
Engineering, University of Rochester,
Rochester, New York, United States
kevin.parker@rochester.edu
(ORCID: 0000-0002-6313-6605)

Abstract—Estimates of speckle statistics of soft tissues provide quantitative measures for characterizing the underlying tissues. The statistical behavior of speckle has been studied for over 100 years, evolving into a number of well-established statistical models such as the Rayleigh. In this study, we propose a new framework for describing the speckle statistics of soft biological tissues, focusing on the presence of *multiscale* (rather than *identical*) scatterers with different shapes (cylindrical, spherical, or irregular inhomogeneities) within tissues. In this framework, we assume that the size distributions of any set of multiscale subresolved scatterers follows a power law distribution, leading to a two-parameter model for describing the underlying speckle statistics (probability density function or PDF), characterized by a key power law exponent and a scale parameter. The derivation under this framework results in the Burr distribution, which has not previously been employed in the field of medical imaging. We tested this hypothesis using 3D simulations of ultrasound scans from multiscale cylindrical or spherical scattering structures, and ultrasound scans from *in vivo* and *ex vivo* soft tissues. The Burr distributions provided promising results for describing speckle statistics in simulations and tissue scans, with its two parameters showing sensitivity to the changes in scattering media.

Keywords—Speckle statistics, ultrasound, Burr distribution, power law, multiscale scatterers, soft tissues

I. INTRODUCTION

In medical ultrasound, the mathematical treatment of speckle pattern has developed substantially over the last 40 years and has developed into a rich set of models for the statistics of backscattered echoes from tissues. These models include the classical Rayleigh distribution [1], the K-distribution [2], a Rician distribution [3], the Nakagami distribution [4] and other advanced models [5] with continuing applications to a variety of clinical targets. These models describe the speckle first order statistics which is the probability distribution function (PDF) of envelope of echo amplitudes. The key assumption in the classical models relies on the presence of many random *identical* scatterers within tissues.

In this study, we propose a new framework as an alternative approach for describing the speckle statistics, focusing on the presence of *multiscale* (rather than *identical*) scatterers with different shapes (cylindrical, spherical or

irregular inhomogeneities) within soft tissues [6-9]. In this framework, we assume that the size distributions of any set of multiscale subresolved scatterers (smaller than the resolution sample volume of the imaging system, so their exact shape and size is not resolved) follows a power law distribution, leading to a two-parameter model for describing the underlying speckle statistics, in the form of a PDF.

II. THEORY

The key assumptions and formulas used in deriving the first order statistics of speckle from this novel framework are explained in detail in [7, 9]. Summarizing the main points, a generalized pair of conditions sufficient for producing the Burr distributions of echo amplitudes are presented as following:

a) We assume that the number density of multiscale subresolved scatterers within the medium goes as power law with the scatterer size a , $N[a] = N_0/a^b$, in which b is the power law parameter and N_0 is a constant. Note that this is consistent with the power law PDF for size distribution of scatterers (denoted as $P[a]$) in (1), in which a_{min} is the scatterer size associated with the smallest subresolved scatterer.

$$P[a] = \left(\frac{(b-1)}{a_{min}} \left(\frac{a}{a_{min}} \right)^{-b} \right) \quad (1)$$

b) It is plausibly assumed that the echo intensity linearly increases with scatterer size, $I[a] = I_0(a - a_{min})$, as a first order approximation over some range which results in the echo amplitude approximated as (2).

$$A[a] = A_0 \sqrt{(a - a_{min})} \quad (2)$$

Applying the general theory of transformed distributions according to (3) using (1) and (2) results in obtaining the distribution of echo amplitude, derived in (4). Equation (4) is a four-parameter model which can be further simplified into a two-parameter model by normalizing the equation and introducing l as a scale factor, $l = A_0 \sqrt{a_{min}}$. The simplified equation presented in (5) is a Burr Type XII distribution [10], (with its third parameter, c , being equal to 2), which has not

been employed in the context of medical imaging before.

$$P[A] = \frac{1}{dA/da} P[a] \quad (3)$$

$$P[A] = \frac{2N_0 A}{A_0^2 \left[\left(\frac{A}{A_0} \right)^2 + a_{min} \right]^b} \quad (4)$$

$$P_n[A] = \frac{2A(b-1)}{l^2 \left[\left(\frac{A}{l} \right)^2 + 1 \right]^b} \quad (5)$$

We propose that the Burr distribution in (5) is the expected normalized histogram distribution of echo amplitudes from ultrasound (as well as optical coherence tomography [11]) scan data from soft tissues with the key power law parameter b . A key feature separating the Burr PDF from classical speckle models such as Rayleigh model is its long power law tail at higher amplitudes [9].

III. METHODS

We aim to test the proposed novel framework for describing ultrasound speckle statistics and evaluate the sensitivity of the two underlying parameters in the Burr model to the changes in the scattering structure in 3D simulations and also ultrasound scan data of soft tissues.

A. 3D simulations of multiscale scattering media: cylindrical and spherical scatterers

Focusing on the presence of multiscale scatterers following a power law distribution with their characteristic length, two sets of 3D simulations of scattering media (to model a 3D block of soft biological tissue) are performed in the k-Wave toolbox in MATLAB [12] based on a specific scatterer shape: (i) cylindrical (to model vessels as scattering sites), and (ii) spherical scatterers. **Fig. 1** shows the 3D orientations of multiscale cylindrical and spherical scatterers with different radii (a few scatterers are shown in each case). For each scatterer shape, a number of different scatterer distribution conditions is simulated based on varying N_0 and b ($N[a] = N_0/a^b$). For the background and scatterers, the speed of sound is set to 1540 m/s and 1500 m/s, respectively. The absorption coefficient is set to a small value, with a low attenuation of 0.004 dB/cm/MHz to simplify the comparison across different depths. A linear array transducer model is implemented in k-Wave, excited by a two-cycle toneburst signal with a frequency of 4 MHz. The dimensions of the 3D domain along x , y , and z are 15 mm, 13 mm, 3 mm, respectively, with uniform mesh sizes of approximately 0.069 mm. The computational time step is set to satisfy the Courant-Friedrichs-Lewy (CFL) criteria, $CFL = (c_0 \Delta t / \Delta x) \leq 0.3$ [13].

B. Ultrasound scans of soft tissues

We examine different *in vivo* and *ex vivo* ultrasound scan data of soft tissues including rat liver and human placentae. *In vivo* rat experiments were reviewed and approved by the Institutional Animal Care and Use Committee of Pfizer, Inc., Connecticut, where the ultrasound radiofrequency (RF) data

of normal and fibrotic rat livers were acquired using a Vevo 2100 (VisualSonics, Toronto, CA) scanner and a 21-MHz center frequency transducer (MS250, VisualSonics, Toronto, CA). *Ex vivo* human placenta experiments were reviewed and approved by the University of Rochester Research Subjects Review Board (RSRB). *Ex vivo* human placenta scanning were performed with placentae in a water bath at physiologic temperature, both before and after reestablishing perfusion of the fetal vasculature. RF data were obtained at

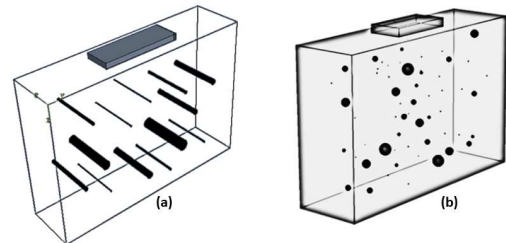


Fig. 1. Multiscale scatterers for the simulation study. (a) Cylindrical and (b) spherical scatterers.

center frequency of 4 MHz using a Siemens S3000 scanner (Siemens Medical Solutions, Malvern, PA, USA) and a L4 linear probe (Siemens Medical Solutions, Malvern, PA, USA).

IV. RESULTS

A. Simulations

Fig. 2 represents the results of four simulation cases from cylindrical and spherical power law multiscale scattering media. The top row shows the 2D view from the middle plane within the 3D domain, the middle row shows the corresponding ultrasound B-scan, and the bottom row demonstrates the speckle statistics of ultrasound echo amplitude fitted to the Burr distribution as derived in (5). In this figure, (a) and (b) are examples of cylindrical scatterer cases and (c) and (d) are spherical scatterer cases, having different scatterer number densities with the generating power law parameter $b = 2.2$. Lower scatterer densities resulted in some anechoic regions within the corresponding B-scan as observed in (a) and (c). It is observed that the Burr distribution describes the ultrasound speckle statistics from power law multiscale scattering media with a reasonable accuracy ($R^2 > 0.98$). Also, it is observed that the Burr distribution shows sensitivity to the changes in scatterer number densities. This sensitivity is further demonstrated by the summary of all fitting results from simulation cases for cylindrical and spherical scattering media shown in **Fig. 3 (a)** and **(b)**, respectively, fitted to the Burr distribution. In this figure, the variation of the Burr power law parameter which quantifies ultrasound speckles is shown on the vertical axis, denoted by \hat{b} to distinguish it from the power law parameter b employed for generating scattering media (represented as distinct colors in these figures), and the N_0 parameter is marked on the horizontal axes. The figures show that the Burr power law parameter increases with scatterer number density

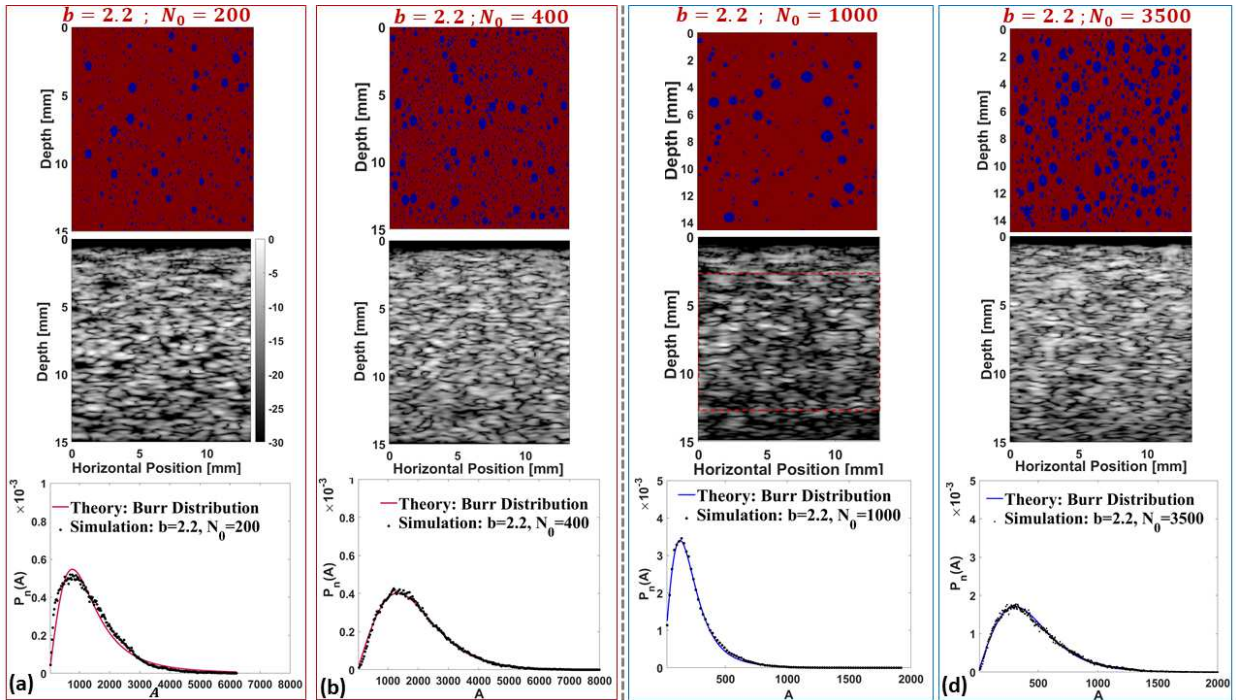


Fig. 2. Top row: 2D view of scattering structure in middle plane, Middle row: B-scan, and bottom row: the speckle statistics fitted to the Burr distribution. (a) and (b) show two different cylindrical scatterer cases, (c) and (d) illustrate two different spherical scatterer cases.

densities by variations in N_0 or b . In these figures, the error bars show the results from different realizations of random scatterer distributions within the domain for a specific set of b and N_0 to show the repeatability of the results.

B. Soft tissues

Fig. 4 shows the results of applying the Burr distribution to soft biological tissues. In this figure, (a) and (b) are the Burr results for *in vivo* rat liver scan data in normal and fibrotic conditions, respectively and (c) and (d) represent the Burr results for *ex vivo* human placenta before perfusion and after introduction of a vasoconstrictive agent in the perfused state, respectively. The corresponding Burr fitting results are shown in **Table 1**. We observe that the Burr distribution describes the ultrasound speckle statistics of different soft biological tissues with a reasonable accuracy and also, its two underlying parameters, \hat{b} and l , show sensitivity to the changes in tissue pathology.

These figures show an example frame from each scanned subject drawn from the ultrasound scan data, It should be noted that these observations, i.e., the excellent Burr goodness-of-fit as well as the sensitivity of Burr parameters to the changes in tissue pathology, were observed when other

Table 1. The Burr fitting results for *in vivo* rat liver and *ex vivo* human placenta.

Case	\hat{b}	l	R^2
Normal rat liver	3.34	279.3	0.998
Fibrotic rat liver	6.23	1523.8	0.992
Placenta before perfusion	3.8	6488	0.9989
Placenta in vasoconstriction	5.2	9966	0.997

frames and other liver or placenta subjects were analyzed. For rat liver, a more comprehensive analysis of different frames and different scanned subjects using the Burr distribution is reported in [14, 15].

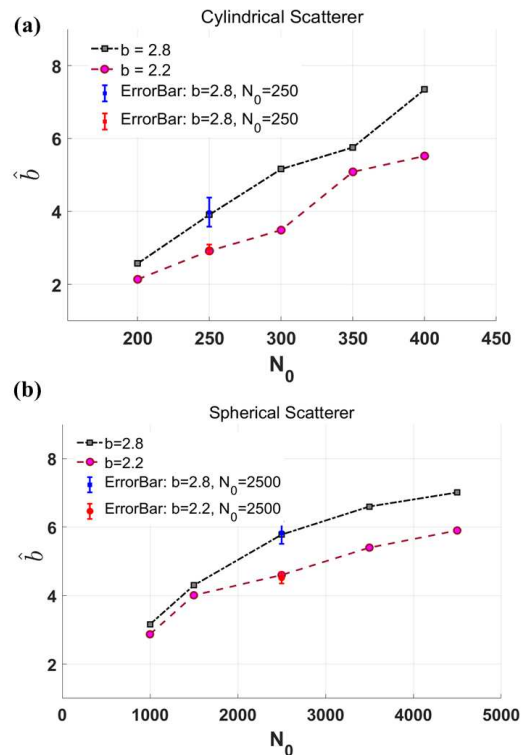


Fig. 3. Summary of simulations Burr parameters for (a) cylindrical and, (b) spherical scatterers.

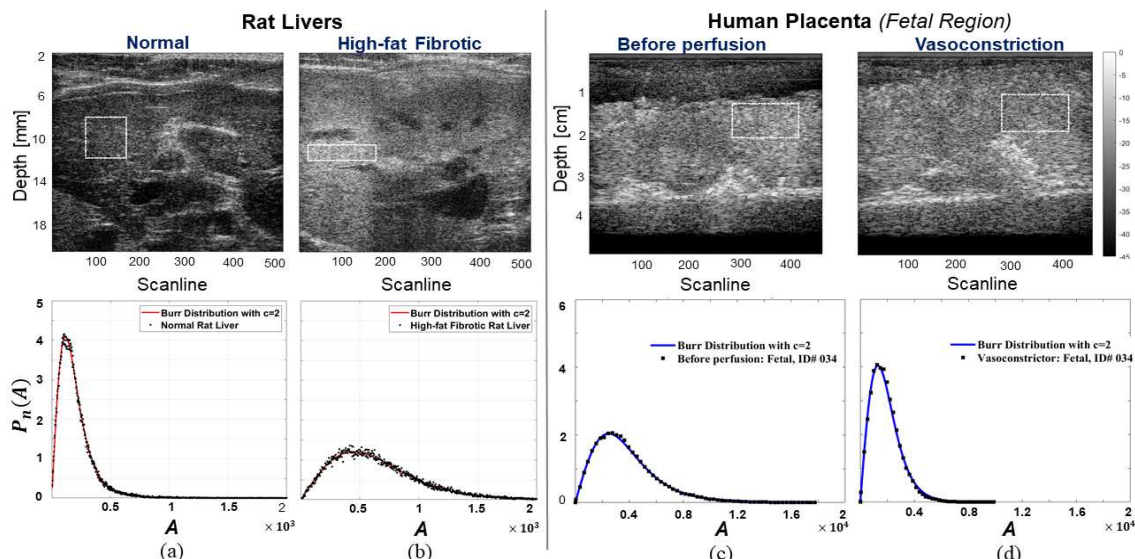


Fig. 4. Top row: B-scan, **bottom row:** speckle statistics fitted to the Burr distribution for (a) normal rat liver, (b) fibrotic rat liver scan data *in vivo*; (c) *ex vivo* human placenta before perfusion (d) *ex vivo* human placenta in vasoconstriction.

V. CONCLUSION

In this study, a new hypothesis for describing the ultrasound first order speckle statistics, i.e., the PDF of the envelope of echo amplitude, is presented and its application and accuracy is tested for a series of ultrasound speckle data from 3D computational imaging of power law multiscale scattering structures, for *in vivo* rat liver ultrasound scan data in normal and fibrotic conditions as well as for *ex vivo* human placenta scan data before perfusion and in perfused, vasoconstricted states. It is shown that the Burr distribution shows promising results in describing the ultrasound speckle first order statistics and its two parameters may have potential for being employed as biomarkers.

ACKNOWLEDGMENT

This work was supported by National Institutes of Health grants R21EB025290 and R21AG070331. The authors thank Terri A. Swanson and Theresa Tuthill from Pfizer Inc. for providing the *in vivo* rat liver scan data.

REFERENCES

- [1] C.B. Burckhardt, Speckle in ultrasound B-mode scans, *IEEE Transactions on Sonics and ultrasonics* 25(1) (1978) 1-6.
- [2] E. Jakeman, R. Tough, Generalized K distribution: a statistical model for weak scattering, *JOSA A* 4(9) (1987) 1764-1772.
- [3] M.F. Insana, R.F. Wagner, B.S. Garra, D.G. Brown, T.H. Shawker, Analysis of ultrasound image texture via generalized Rician statistics, *Optical Engineering* 25(6) (1986) 743-748.
- [4] P.M. Shankar, Ultrasonic tissue characterization using a generalized Nakagami model, *IEEE transactions on ultrasonics, ferroelectrics, and frequency control* 48(6) (2001) 1716-1720.

- [5] R.W. Prager, A.H. Gee, G.M. Treece, L.H. Berman, Analysis of speckle in ultrasound images using fractional order statistics and the homodyned k-distribution, *Ultrasonics* 40(1-8) (2002) 133-137.

- [6] K. Parker, Shapes and distributions of soft tissue scatterers, *Physics in Medicine & Biology* 64(17) (2019) 175022.

- [7] K.J. Parker, The first order statistics of backscatter from the fractal branching vasculature, *The Journal of the Acoustical Society of America* 146(5) (2019) 3318-3326.

- [8] K.J. Parker, S.S. Poul, Burr, Lomax, Pareto, and logistic distributions from ultrasound speckle, *Ultrasonic imaging* 42(4-5) (2020) 203-212.

- [9] K.J. Parker, S.S. Poul, Generalized formulations producing a Burr distribution of speckle statistics, *Journal of Medical Imaging* 9(2) (2022) 023501.

- [10] I.W. Burr, Cumulative frequency functions, *The Annals of mathematical statistics* 13(2) (1942) 215-232.

- [11] R.G. Gary, W. Song, M. Nedergaard, J.P. Rolland, K.J. Parker, Speckle statistics of cortical brain tissue in optical coherence tomography, *Biomedical Applications of Light Scattering XII*, SPIE, 2022, pp. 9-14.

- [12] B.E. Treeby, B.T. Cox, k-Wave: MATLAB toolbox for the simulation and reconstruction of photoacoustic wave fields, *Journal of biomedical optics* 15(2) (2010) 021314.

- [13] K.J. Parker, S.S. Poul, Speckle from branching vasculature: dependence on number density, *Journal of Medical Imaging* 7(2) (2020) 027001.

- [14] J. Baek, S.S. Poul, L. Basavarajappa, S. Reddy, H. Tai, K. Hoyt, K.J. Parker, Clusters of ultrasound scattering parameters for the classification of steatotic and normal livers, *Ultrasound in Medicine & Biology* 47(10) (2021) 3014-3027.

- [15] J. Baek, S.S. Poul, T.A. Swanson, T. Tuthill, K.J. Parker, Scattering signatures of normal versus abnormal livers with support vector machine classification, *Ultrasound in Medicine & Biology* 46(12) (2020) 3379-3392.